Magnified time-domain ghost imaging

Piotr Ryczkowski, Margaux Barbier, Ari T. Friberg, John M. Dudley, and Goëry Genty

Citation: APL Photonics **2**, 046102 (2017); doi: 10.1063/1.4977534
View online: http://dx.doi.org/10.1063/1.4977534
View Table of Contents: http://aip.scitation.org/toc/app/2/4
Published by the American Institute of Physics

Articles you may be interested in

Development of ultrafast time-resolved dual-comb spectroscopy
APL Photonics **2**, 041301041301 (2017); 10.1063/1.4976730

Why I am optimistic about the silicon-photonic route to quantum computing
APL Photonics **2**, 030901030901 (2017); 10.1063/1.4976737

Electro-opto-mechanical radio-frequency oscillator driven by guided acoustic waves in standard single-mode fiber
APL Photonics **2**, 041303041303 (2017); 10.1063/1.4977904

A tunable waveguide-coupled cavity design for scalable interfaces to solid-state quantum emitters
APL Photonics **2**, 046103046103 (2017); 10.1063/1.4978204

Ultraviolet photoluminescence in Gd-doped silica and phosphosilicate fibers
APL Photonics **2**, 046101046101 (2017); 10.1063/1.4976304

Ultra-compact visible chiral spectrometer with meta-lenses
APL Photonics **2**, 036103036103 (2017); 10.1063/1.4974259

Magnified time-domain ghost imaging

Piotr Ryczkowski,[1,a] Margaux Barbier,[1,b] Ari T. Friberg,[2] John M. Dudley,[3] and Goëry Genty[1]
[1]*Optics Laboratory, Tampere University of Technology, Tampere, Finland*
[2]*Department of Physics and Mathematics, University of Eastern Finland, Joensuu, Finland*
[3]*Institut FEMTO-ST, UMR 6174 CNRS-Université de Franche-Comté, Besançon, France*

(Received 24 November 2016; accepted 14 February 2017; published online 8 March 2017)

Ghost imaging allows the imaging of an object without directly seeing this object. Originally demonstrated in the spatial domain, it was recently shown that ghost imaging can be transposed into the time domain to detect ultrafast signals, even in the presence of distortion. We propose and experimentally demonstrate a temporal ghost imaging scheme which generates a 5× magnified ghost image of an ultrafast waveform. Inspired by shadow imaging in the spatial domain and building on the dispersive Fourier transform of an incoherent supercontinuum in an optical fiber, the approach overcomes the resolution limit of standard time-domain ghost imaging generally imposed by the detectors speed. The method can be scaled up to higher magnification factors using longer fiber lengths and light source with shorter duration. © *2017 Author(s). All article content, except where otherwise noted, is licensed under a Creative Commons Attribution (CC BY) license (http://creativecommons.org/licenses/by/4.0/).* [http://dx.doi.org/10.1063/1.4977534]

I. INTRODUCTION

Ghost imaging retrieves the image of an object from the correlation between a spatially resolved structured illumination pattern and the total intensity transmitted through (or reflected by) the object.[1,2] Originally developed to test the EPR paradox using entangled photon sources,[2–6] the concept has subsequently been expanded to classical spatially incoherent light sources[2,7–11] and more recently to pre-programmed illumination with a spatial light modulator.[12] More advanced schemes based on multiplexing have also been demonstrated, to reduce the acquisition time[13] or to image objects which vary slowly with time.[14] Compared to standard imaging techniques, a unique property of ghost imaging is its intrinsic insensitivity to distortions that may occur between the object and the single-pixel detector that only measures the total transmitted (or reflected) intensity.[15,16] This specific feature has made ghost imaging particularly attractive for many applications ranging from microscopy and compressive sensing to LIDAR or atmospheric sensing.

Very recently, taking advantage of the space-time propagation correspondence in optics,[17–20] ghost imaging has been transposed into the time domain to produce the image of an ultrafast signal by correlating, in time, the intensity of two temporally incoherent light beams, neither of which independently carried information about the signal.[21] Significantly, it was also demonstrated that the technique is insensitive to distortion that the signal may experience between the object and the detector, e.g., due to dispersion, nonlinearity, or attenuation. Despite the fact that this transposition has opened up novel opportunities for the detection of ultrafast waveforms, an important limitation of ghost imaging in the time-domain that may limit its usability is the finite resolution determined by the fluctuation time of the random light source and/or the speed of the detection system.

Here, we propose a new approach for ghost imaging in the time domain that magnifies the retrieved temporal object and allows overcoming the limited resolution of the original ghost imaging

[a]piotr.ryczkowski@tut.fi
[b]Current address: FOTON Laboratory, CNRS, University of Rennes 1, ENSSAT, 6 Rue de Kerampont, F-22305 Lannion, France.

 © Author(s) 2017

scheme imposed by the finite speed of photodetectors, without the need of using advanced temporal imaging schemes.[22] The approach is inspired by shadow imaging in the spatial domain and builds on the dispersive Fourier transform of the fast random fluctuations of an incoherent supercontinuum (SC) generated by noise-seeded modulation instability. We experimentally demonstrate a factor of five magnification of a temporal object in the form of the transmission of an electro-optic modulator. Higher magnification factors can be obtained by using a longer length of dispersive fiber or shorter initial pulse duration. By proposing a new approach to improve the resolution of time-domain ghost imaging, our results open a new avenue to blindly detect and magnify ultrafast signals.

II. MAGNIFIED TIME-DOMAIN GHOST IMAGING USING DISPERSIVE FOURIER TRANSFORM

In time-domain ghost imaging, the fast temporal fluctuations of an incoherent light source are divided between a test arm, where a temporal object modulates the intensity fluctuations of the source, and a reference arm where the fluctuations are resolved in real time in the image plane[21] [i.e., the plane of the reference arm detector, see Fig. 1(a)]. By correlating the time-resolved fluctuations from the reference arm with the total (integrated) power transmitted in the test arm, a perfect copy of the temporal object can be retrieved. The temporally incoherent light source may be a quasi-continuous wave source with a fluctuation time inversely proportional to the source bandwidth or a pulsed source with large intensity variations both within a single pulse and from pulse to pulse.[23] The correlation is calculated from multiple measurements synchronized with the temporal object. Note that the average intensity value of the source over the measurement time window does not affect the ghost image, however if the magnitude of the source intensity fluctuations varies over the duration of the temporal object (which can be the case especially for a pulsed source), the ghost image is distorted and requires post-processing correction.[23]

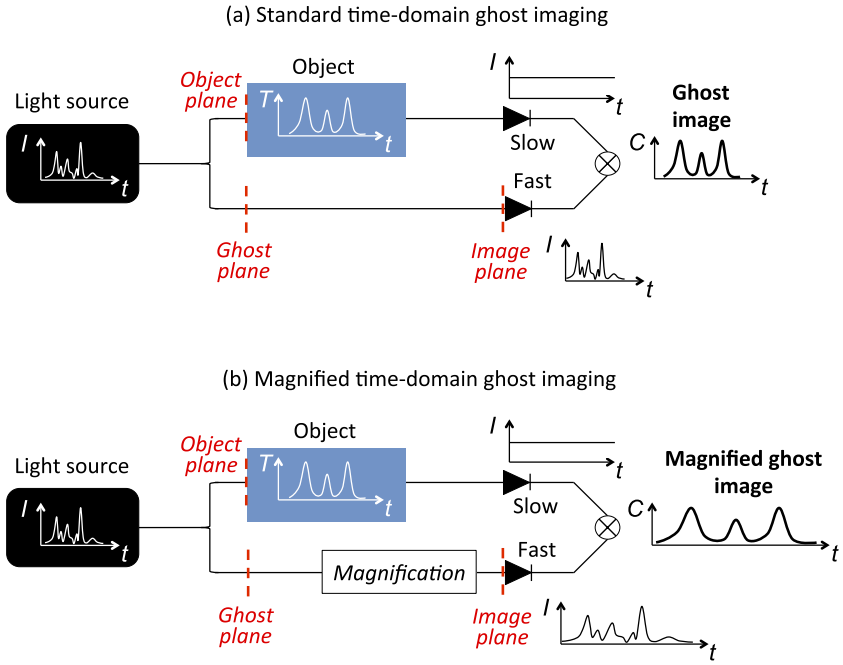

FIG. 1. Operation principle of (a) standard time-domain ghost imaging and (b) magnified time-domain ghost imaging. The ghost plane is defined in the reference arm as the equivalent of the object plane (which is, by definition, located in the test arm), such that the dispersion accumulated by the light between the source and the ghost plane is equal to the dispersion accumulated between the source and the temporal object. I = light intensity. T = transmission of an intensity modulator (= object). C = correlation function.

In order to obtain a magnified ghost image, the temporal fluctuations of the source in the reference arm must be magnified[23] whilst in the test arm one only needs to measure the total (integrated) intensity with no modification compared to standard time-domain ghost imaging [see Fig. 1(b)]. In principle, magnification of the source fluctuations can be obtained using a time lens system.[24–26] However, time lens systems generally require complicated schemes to impose the necessary quadratic chirp onto the signal to be magnified and typically operate only at a fixed repetition rate with limited numerical apertures.

A different approach consists of using a broadband, temporally incoherent light source whose random intensity fluctuations can then be magnified in the reference arm using a simple dispersive fiber. There are of course some constraints which need to be considered. First, the time span ΔT^{GP} of the light source fluctuations in the ghost plane defined as the equivalent of the object plane in the reference arm (see Fig. 1) needs to be longer or equal to that of the duration of the temporal object to be retrieved. Second, the characteristic fluctuation time at the ghost plane (and correspondingly in the object plane) τ_c^{GP} needs to be shorter than the shortest object detail that one wishes to resolve. These criteria can be fulfilled by an incoherent SC source whose spectral fluctuations are converted into the time domain using spectrum-to-time transformation or dispersive Fourier transform as illustrated in Fig. 2, whereby the dispersion of an optical fiber allows separating in time the fluctuations associated with each spectral component.[27,28] The characteristic frequency of the SC spectral fluctuations is well-approximated by $\Delta\omega_c \approx 1/\Delta T_0$, where ΔT_0 is the average duration of the SC pulses. When these spectral fluctuations are converted into the time domain by a dispersive fiber with total dispersion $\beta_2 L_a$, the resulting incoherent pulse source exhibits (intra-pulse) temporal fluctuations $\tau_c^{\mathrm{GP}} \approx |\beta_2| L_a/\Delta T_0$ at the ghost (and object) plane.

The fluctuations from the pulse source are then divided between the test arm, where the temporal object is located, and the reference arm where they are stretched further in a second segment of

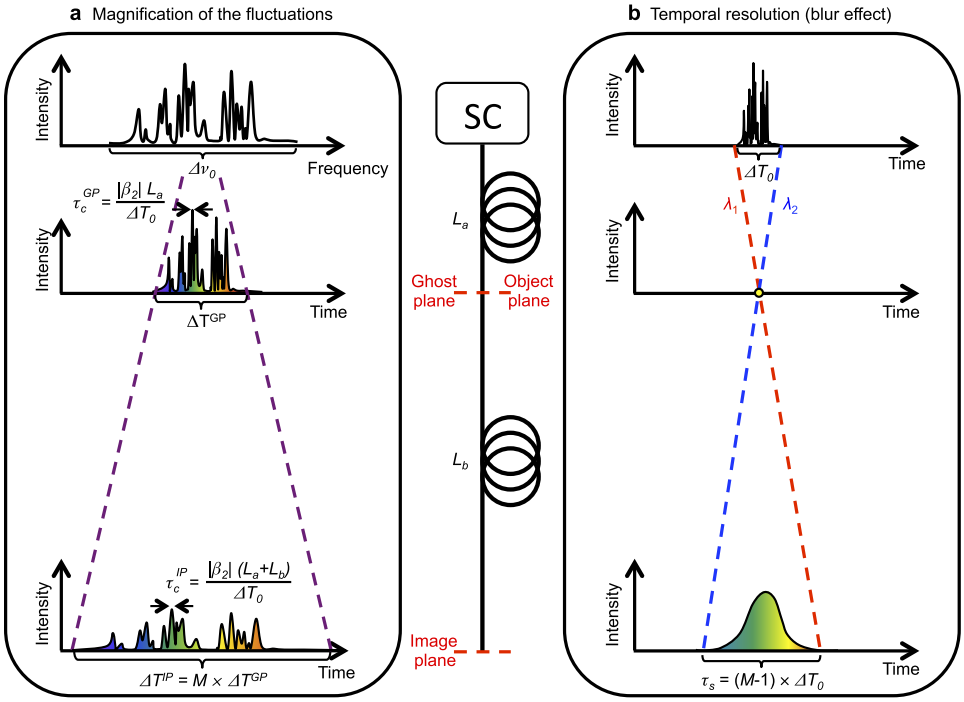

FIG. 2. Spectrum-to-time transformation of the incoherent supercontinuum (SC) as it propagates from the SC source through the dispersive fiber L_a to the ghost and object planes and further through the dispersive fiber L_b to the image plane. (a) Temporal magnification of the intensity fluctuations of the SC. (b) Temporal resolution limit from the finite duration of the SC pulses. ΔT_0 and $\Delta\nu_0$ represent the initial duration and bandwidth of the SC pulses, respectively. ΔT^{GP} and ΔT^{IP} represent the duration of the SC pulses at the ghost and image planes, respectively. τ_c^{GP} and τ_c^{IP} denote the characteristic fluctuation time within each SC pulse at the ghost and image planes, respectively. τ_s is the temporal blur resulting from the different spectral components λ_1 and λ_2 that correspond to the temporal edges of the initial SC pulses and temporally overlap in the ghost plane.

dispersive fiber with total dispersion $\beta_2 L_b$. The fluctuation time at the image plane in the reference arm is then $\tau_c^{IP} \approx |\beta_2|(L_a + L_b)/\Delta T_0$, such that the temporal fluctuations in the reference arm are magnified by a factor $M = (\beta_2 L_a + \beta_2 L_b)/\beta_2 L_a = 1 + L_b/L_a$ compared to the fluctuations in the ghost plane (see Fig. 2(a) and also the supplementary material).

By correlating the magnified random fluctuations measured in the reference arm with the total transmitted intensity through the object in the test arm, one then directly obtains an M-time magnified image of the temporal object, effectively improving the overall resolution of the ghost imaging scheme by the same factor (for a fixed detector bandwidth). The initial duration ΔT_0 of the SC pulses is finite such that each time instant in the ghost plane (and, equivalently in the test arm, each time instant of the object plane) actually includes the contribution from several spectral components. These spectral components propagate to the image plane with different group-velocities due to dispersion [see Fig. 2(b)], which results in a "temporal blur effect" that limits the resolution of the imaging system. The temporal blur is defined as the delay τ_s, in the image plane, between the frequencies corresponding to the temporal edges of the initial SC pulses and contributing to the same time instant in the ghost (and object) plane (see the supplementary material). Basic geometric considerations in Fig. 2(b) show that

$$\tau_s = \frac{L_b}{L_a}\Delta T_0 = (M - 1)\Delta T_0. \tag{1}$$

For each SC pulse i, the oscilloscope records a pair of measurements: the magnified fluctuations $I_{\text{ref}}^{(i)}(t)$ and the total intensity transmitted through the electro-optic modulator $I_{\text{test}}^{(i)}$. This pair is recorded N times and the normalized correlation function which produces the ghost image is then calculated according to

$$C(t) = \frac{\left\langle \Delta I_{\text{ref}}^{(i)}(t) \cdot \Delta I_{\text{test}}^{(i)} \right\rangle}{\sqrt{\left\langle \left[\Delta I_{\text{ref}}^{(i)}(t)\right]^2 \right\rangle \left\langle \left[\Delta I_{\text{test}}^{(i)}\right]^2 \right\rangle}}, \tag{2}$$

where $\langle\rangle$ represents the ensemble average over the N realizations ($i = 1 \ldots N$) and $\Delta I^{(i)} = I^{(i)} - \langle I^{(i)} \rangle$.

III. EXPERIMENTAL SETUP

The experimental setup is illustrated in Fig. 3(a). The light source consists of an incoherent SC followed by a dispersive fiber which performs the dispersive Fourier transform. The incoherent SC with large shot-to-shot spectral fluctuations is generated by injecting 0.5 ns pulses produced by an erbium-doped fiber laser (Keopsys PEFL-KULT) operating at 1547 nm with 100-kHz repetition rate into the anomalous dispersion regime of a 6-m long dispersion-shifted fiber (Corning ITU-T G.655) with zero-dispersion at 1510 nm. The SC generation process is initially triggered by modulation instability which breaks up the long initial pulse into a series of random and shorter pulses. The spectral components of the SC below 1550 nm are filtered out with a long-pass filter to obtain a relatively flat spectrum. The average power of the SC is then reduced with an attenuator (Thorlabs VOA50-FC) to avoid any nonlinear process that may occur during further propagation in an optical fiber. After the spectral filtering stage, the SC has a bandwidth of 80 nm and the average duration of the SC pulses ΔT_0 was measured to be less than 200 ps. Note that the duration of the SC after filtering is shorter than that of the original pump pulses. This is because the SC is not transform-limited, such that filtering out the pump remains effectively remove the undepleted temporal wings of the initial long pulse thus reducing the overall duration.

The spectral fluctuations of the SC are subsequently converted into the time domain through dispersive Fourier transform using an SMF-28 fiber of length $L_a = 2.5$ km and dispersion parameter $\beta_2 = -20$ ps^2/km at 1550 nm. The average duration ΔT^{GP} of the source pulses at the ghost (and object) plane was then measured to be approximately 4 ns. As required, this value exceeds the duration of the temporal object to be measured (see below). The standard deviation of the magnitude of the fluctuations is nearly constant over this time span [see the dotted black curve in the inset of Fig. 3(b)], such that the ghost image will not be distorted. The pulses are then split between the

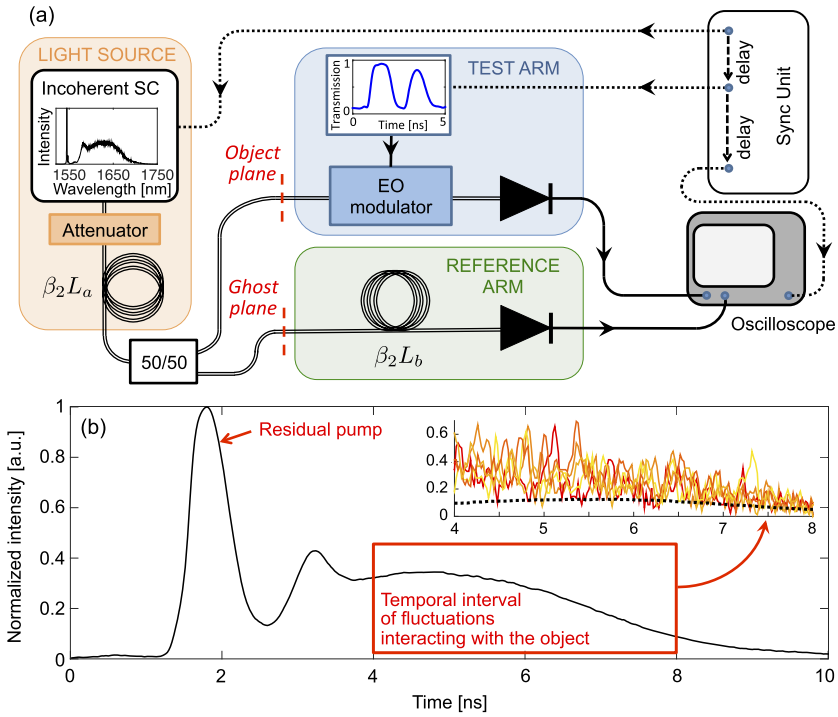

FIG. 3. Magnified time-domain ghost imaging experimental setup. (a) Setup. The synchronization unit allows synchronizing the electric signal driving the transmission function of the electro-optic (EO) modulator with the arrival time of the SC pulse at the modulator and triggering the oscilloscope. The inset in the light source box shows the average SC spectrum as measured with an optical spectrum analyzer with 0.1-nm resolution. (b) Average of 10 000 temporal traces recorded (with a 12.5-GHz InGaAs photodiode, Electro-Optics Technology ET-3500F) at the ghost plane, showing that after propagating in the 2.5-km fiber, the temporal profile of the SC reproduces its spectral shape (spectrum-to-time transformation). Inset: Examples of 5 distinct SC pulse traces recorded at the ghost plane together with the standard deviation (dotted black curve) calculated over 10 000 realizations.

test and reference arms with a 50/50 coupler. In the test arm, the temporal object is the transmission of a zero-chirp 10-GHz-bandwidth electro-optic modulator (Thorlabs LN81S-FC) driven by a programmable nanosecond pulse generator (iC-Haus iC149). It consists of two 0.75-ns pulses with different amplitudes, spanning a total duration of 3.5 ns. In the reference arm, the temporal fluctuations are magnified with an additional dispersive step in an SMF-28 fiber of length $L_b = 10$ km selected to yield an integer magnification factor of 5. Direct measurement of the average duration of the pulses ΔT^{IP} after the additional dispersive step in the reference arm confirmed the 5× increase in the duration to 20 ns.

The detector in the test arm is a 5-GHz InGaAs photodiode (Thorlabs DET08CFC/M) whose response is integrated over 5 ns, such that the effective bandwidth is equal to 0.2 GHz only and the temporal profile of the object cannot be resolved in the test arm. The detector in the reference arm is a 1.2-GHz InGaAs photodiode (Thorlabs DET01CFC). The intensities measured by the two detectors are recorded by a real-time oscilloscope (Tektronix DSA72004). The detection bandwidth was intentionally limited to 625 MHz (with a sampling rate of 6.25 GS/s). Thus, the effective response time of the detection system that measures the fluctuations in real time in the reference arm is $\tau_d = 1.6$ ns.

IV. RESULTS AND DISCUSSION

The correlation $C(t)$ calculated over $N = 100\,000$ SC pulses allows us to construct a ghost image magnified by a factor of $M = 5$, as shown in Fig. 4. In this figure, we compare the ghost image with the original temporal object measured directly with a continuous-wave laser and 5-GHz photodiode (Thorlabs DET08CFC/M) and magnified 5× through post-processing. We can see very good

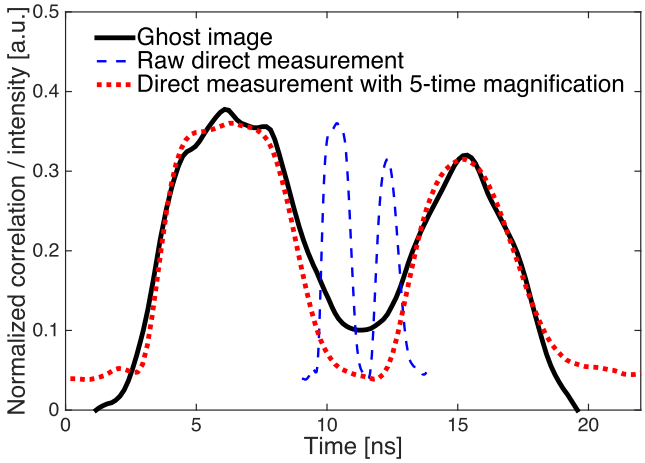

FIG. 4. Magnified ghost image obtained by correlating the signals of the test and reference arms over 100 000 supercontinuum pulses (solid black line). For comparison, the direct measurement of the temporal object (with a 5-GHz detector) is shown before (dashed blue line) and after (dotted red line) post-processed 5-time magnification.

agreement, both in terms of duration and amplitude ratios of the object pulses, confirming the 5-time magnification factor of the object duration in the ghost imaging configuration. The slight distortion of the magnified image is caused by the blur effect of the magnifying scheme.

The temporal resolution τ_R of the imaging scheme is determined by the combination of (i) the time response τ_d of the detection system, (ii) the characteristic time τ_c^{GP} of the random intensity fluctuations in each pulse at the ghost (or object) plane, and (iii) the initial duration ΔT_0 of each SC pulse (i.e., before the spectrum-to-time transformation) which induces a temporal blur $\tau_s = (M-1)\Delta T_0$ in the image plane (see Fig. 2(b) and also the supplementary material). The overall resolution can then be approximated as

$$\tau_R = \sqrt{\left(\frac{\tau_d}{M}\right)^2 + \left(\tau_c^{\mathrm{GP}}\right)^2 + \left(\frac{\tau_s}{M}\right)^2}. \tag{3}$$

Note that in writing Eq. (3) we account for the fact that the fluctuations of the light source are magnified by a factor M, effectively improving the resolution τ_d of the detection system by the same factor. The resolution of the magnified ghost imaging system is illustrated in Fig. 5 as a function of

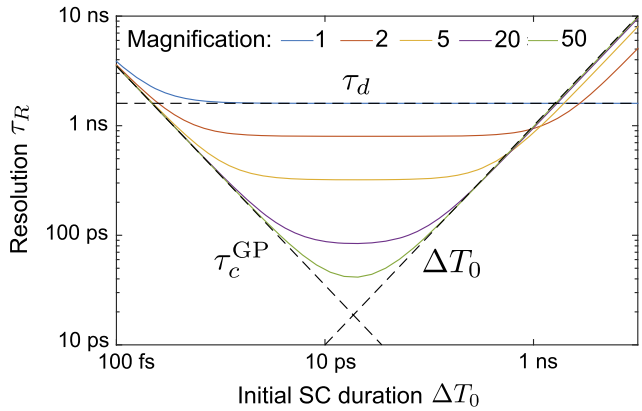

FIG. 5. Resolution of the magnified ghost imaging setup as a function of the supercontinuum initial duration and for various magnification factors. The time response of the detection system in the reference arm τ_d is taken to be 1.6 ns, and the characteristic fluctuation time of the supercontinuum pulses in the ghost plane τ_c^{GP} is set equal to 50 $ps^2/\Delta T_0$ (consistent with our experimental parameters). The dashed lines illustrate the different factors that limit the resolution (detector speed τ_d, characteristic time of fluctuations at the ghost plane τ_c^{GP}, and initial duration of the SC pulses ΔT_0).

the initial SC pulse duration ΔT_0 and for different values of the magnification factor. We can see that for short initial durations ($\leq$1 ps), it is the fluctuation time of the light source at the ghost (or object) plane τ_c^{GP} that determines the overall resolution of the imaging system. In contrast, for long SC pulse durations ($\geq$100 ps), it is the time delay τ_s between the SC frequencies at the image plane that sets the temporal resolution. The response time of the detection system τ_d only has an effect for small magnification factors. The temporal resolution τ_R in the results of Fig. 4 is estimated to be 360 ps, determined both by the resolution of the detection system in the reference arm $\tau_d = 1.6\ ns$ and by the temporal spreading of the SC frequencies in the image plane $\tau_s \approx 0.8$ ns, the fluctuation time of the SC pulses at the ghost (or object) plane $\tau_c^{GP} \approx 0.3$ ps having a negligible influence. The resolution of the imaging system is therefore improved by a factor τ_d/τ_R approximately equal to the magnification factor M compared to the standard ghost imaging setup.

The optimum resolution of the scheme can be achieved for a magnification factor $M >> 1$ and is equal to $\sqrt{2|\beta_2|L_a}$ (corresponding to an initial SC duration $\Delta T_0 = \sqrt{|\beta_2|L_a}$). This implies that one should use a short segment of dispersive fiber to convert the spectral fluctuations of the SC to the time-domain. However, one should also bear in mind that the fiber segment should be long enough so as to image the full temporal object. It is then clear that an incoherent SC source with a short (average) initial pulse duration ΔT_0 and large bandwidth would be ideal for the scheme demonstrated here.

V. CONCLUSION

Using dispersive spectrum-to-time transformation of the fluctuations of an incoherent supercontinuum, we have demonstrated ghost imaging with magnification in the time domain. This approach increases the effective fluctuation time of the light source and thus overcomes the limited resolution of the standard time-domain ghost imaging generally imposed by the speed of the detection system. Large magnification factors can be obtained using a pulsed light source of short duration. We emphasize that the magnified approach demonstrated here is also insensitive to any distortion that would affect the light field after the object. Our results open novel perspectives for dynamic imaging of ultrafast waveforms with potential applications in communications and spectroscopy.

SUPPLEMENTARY MATERIAL

See supplementary material for description of the analogy between dispersive spectrum-to-time transformation in the temporal domain and shadow imaging in the spatial domain.

ACKNOWLEDGMENTS

G.G. and A.T.F gratefully acknowledge support from the Academy of Finland (Projects No. 267576 and 298463). J.M.D. acknowledges the ERC project MULTIWAVE. The project has further received funding from the European Union Horizon 2020 research and innovation programme under Grant Agreement No. 722380.

[1] B. I. Erkmen and J. H. Shapiro, "Ghost imaging: From quantum to classical to computational," Adv. Opt. Photonics **2**, 405–450 (2010).
[2] R. S. Bennink, B. I. Bentley, R. W. Boyd, and J. C. Howell, "Quantum and classical coincidence imaging," Phys. Rev. Lett. **92**, 033601 (2004).
[3] D. N. Klyshko, "A simple method of preparing pure states of an optical field, of implementing the einstein-podolsky-rosen experiment, and of demonstrating the complementarity principle," Sov. Phys. Usp. **31**, 74–85 (1988).
[4] D. N. Klyshko, "Combine EPR and two-slit experiments: Interference of advanced waves," Phys. Lett. A **132**, 299–304 (1988).
[5] T. B. Pittman, Y. H. Shih, D. V. Strekalov, and A. V. Sergienko, "Optical imaging by means of two-photon quantum entanglement," Phys. Rev. A **52**, R3429 (1995).
[6] A. F. Abouraddy, B. E. A. Saleh, A. V. Sergienko, and M. Teich, "Role of entanglement in two-photon imaging," Phys. Rev. Lett. **87**, 123602 (2001).
[7] R. S. Bennink, S. J. Bentley, and R. W. Boyd, "'Two-photon' coincidence imaging with a classical source," Phys. Rev. Lett. **89**, 113601 (2002).
[8] G. Scarcelli, V. Berardi, and Y. Shih, "Can two-photon correlation of chaotic light be considered as correlation of intensity fluctuations?," Phys. Rev. Lett. **96**, 063602 (2006).

[9] R. Meyers, K. S. Deacon, and Y. Shih, "Ghost-imaging experiment by measuring reflected photons," Phys. Rev. A **77**, 041801 (2008).
[10] T. Shirai, T. Setälä, and A. T. Friberg, "Ghost imaging of phase objects with classical incoherent light," Phys. Rev. A **84**, 041801 (2011).
[11] C. Zhang, S. Guo, J. Cao, J. Guan, and F. Gao, "Object reconstitution using pseudo-inverse for ghost imaging," Opt. Express **22**, 30063–30073 (2014).
[12] B. Sun, M. P. Edgar, R. Bowman, L. E. Vittert, S. Welsh, A. Bowman, and M. J. Padgett, "3d computational imaging with single-pixel detectors," Science **340**, 844–847 (2013).
[13] D.-J. Zhang, H.-G. Li, Q.-L. Zhao, S. Wang, H.-B. Wang, J. Xiong, and K. Wang, "Wavelength-multiplexing ghost imaging," Phys. Rev. A **92**, 013823 (2015).
[14] F. Devaux, P.-A. Moreau, S. Denis, and E. Lantz, "Computational temporal ghost imaging," Optica **3**, 698–701 (2016).
[15] F. Ferri, D. Magatti, A. Gatti, M. Bache, E. Brambilla, and L. A. Lugiato, "High-resolution ghost image and ghost diffraction experiments with thermal light," Phys. Rev. Lett. **94**, 183602 (2005).
[16] R. E. Meyers, K. S. Deacon, and Y. Shih, "Turbulence-free ghost imaging," Appl. Phys. Lett. **98**, 111115 (2011).
[17] P. Tournois, "Analogie optique de la compression d'impulsions," C. R. Acad. Sci. **258**, 3839 (1964).
[18] B. H. Kolner and M. Nazarathy, "Temporal imaging with a time lens," Opt. Lett. **14**, 630–632 (1989).
[19] B. H. Kolner, "Space-time duality and the theory of temporal imaging," IEEE J. Quantum Electron. **30**, 1951–1963 (1994).
[20] R. Salem, M. A. Foster, and A. L. Gaeta, "Application of space-time duality to ultrahigh-speed optical signal processing," Adv. Opt. Photonics **5**, 274–317 (2013).
[21] P. Ryczkowski, M. Barbier, A. T. Friberg, J. M. Dudley, and G. Genty, "Ghost imaging in the time domain," Nat. Photonics **10**, 167–170 (2016).
[22] M. Närhi, B. Wetzel, C. Billet, S. Toenger, T. Sylvestre, J.-M. Merolla, R. Morandotti, F. Dias, G. Genty, and J. M. Dudley, "Real-time measurements of spontaneous breathers and rogue wave events in optical fibre modulation instability," Nat. Commun. **7**, 13675 (2016).
[23] T. Shirai, T. Setälä, and A. T. Friberg, "Temporal ghost imaging with classical non-stationary pulsed light." J. Opt. Soc. Am. B **27**, 2549–2555 (2010).
[24] R. Salem, M. A. Foster, A. C. Turner, D. F. Geraghty, M. Lipson, and A. L. Gaeta, "Optical time lens based on four-wave mixing on a silicon chip," Opt. Lett. **33**, 1047–1049 (2008).
[25] M. A. Foster, R. Salem, D. F. Geraghty, A. C. Turner-Foster, M. Lipson, and A. L. Gaeta, "Silicon-chip-based ultrafast optical oscilloscope," Nature **456**, 81–84 (2008).
[26] J. Schröder, F. Wang, A. Clarke, E. Ryckeboer, M. Pelusi, M. A. Roelens, and B. J. Eggleton, "Aberration-free ultra-fast optical oscilloscope using a four-wave mixing based time-lens," Opt. Commun. **283**, 2611–2614 (2010).
[27] D. R. Solli, G. Herink, B. Jalali, and C. Ropers, "Fluctuations and correlations in modulation instability," Nat. Photonics **6**, 463–468 (2012).
[28] K. Goda and B. Jalali, "Dispersive fourier transformation for fast continuous single-shot measurements," Nat. Photonics **7**, 102–112 (2013).